Eur Radiol (2018) 28:708–717
DOI 10.1007/s00330-017-4980-z

MAGNETIC RESONANCE

Invasive placenta previa: Placental bulge with distorted uterine outline and uterine serosal hypervascularity at 1.5T MRI – useful features for differentiating placenta percreta from placenta accreta

Xin Chen[1] · Ruiqin Shan[2] · Lianxin Zhao[3] · Qingxu Song[4] · Changting Zuo[5] · Xinjuan Zhang[1] · Shanshan Wang[1] · Honglu Shi[1] · Fei Gao[1] · Tianyi Qian[6] · Guangbin Wang[1] · Catherine Limperopoulos[7,8]

Received: 16 March 2017 / Revised: 28 May 2017 / Accepted: 6 July 2017 / Published online: 2 August 2017

Abstract

Objectives To characterise MRI features of invasive placenta previa and to identify specific features for differentiating placenta percreta (PP) from placenta accreta (PA).

Methods Forty-five women with PP and 93 women with PA who underwent 1.5T placental MRI were included. Two radiologists independently evaluated the MRI features of invasive placenta previa, including our novel type of placental bulge (i.e. placental bulge type-II, characterized by placental bulge with distorted uterine outline). Pearson's chi-squared or Fisher's two-sided exact test was performed to compare the MRI features between PP and PA. Logistic stepwise regression analysis and the area under the receiver operating characteristic curve (AUC) were performed to select the optimal features for differentiating PP from PA.

Results Significant differences were found in nine MRI features between women with PP and those with PA ($P < 0.05$). Placental bulge type-II and uterine serosal hypervascularity were independently associated with PP (odds ratio = 48.618, $P < 0.001$; odds ratio = 4.165, $P = 0.018$ respectively), and the combination of the two MRI features to distinguish PP from PA yielded an AUC of 0.92 for its predictive performance.

Conclusion Placental bulge type-II and uterine serosal hypervascularity are useful MRI features for differentiating PP from PA.

Key Points

- *Placental bulge type-II demonstrated the strongest independent association with PP.*
- *Uterine serosal hypervascularity is a useful feature for differentiating PP from PA.*
- *MRI features associated with abnormal vessels increase the risk of massive haemorrhage.*

Keywords Placenta percreta · Placenta increta · Placenta accreta · Magnetic resonance imaging · Prenatal diagnosis

Abbreviations

AIP	Abnormal invasive placenta

✉ Guangbin Wang
wgb7932596@hotmail.com

[1] Department of MR, Shandong Medical Imaging Research Institute, Shandong University, 324, Jingwu Road, Jinan, Shandong 250021, People's Republic of China

[2] Department of Obstetrics, Jinan Maternity and Child Care Hospital, 2 Jianguoxiaojingsan Road, Jinan 250001, People's Republic of China

[3] Department of Radiology, Qilu Hospital of Shandong University, 107, Wenhua Xi Road, Jinan, Shandong 250012, People's Republic of China

[4] Department of Radiation Oncology, Qilu Hospital of Shandong University, 107, Wenhua Xi Road, Jinan, Shandong 250012, People's Republic of China

[5] Department of Obstetrics and Gynaecology, Shandong Provincial Hospital Affiliated to Shandong University, 107, Wenhua Xi Road, Jinan, Shandong 250012, People's Republic of China

[6] Siemens Healthcare, MR Collaborations NE Asia, Beijing 100000, People's Republic of China

[7] Division of Diagnostic Imaging and Radiology, Children's National Health System, Washington, DC 20010, USA

[8] Department of Radiology, George Washington University School of Medicine, Washington, DC 20052, USA

AUC	Area under the receiver operating characteristic curve
MRI	Magnetic resonance imaging
NPV	Negative predictive value
PA	Placenta accreta
PP	Placenta percreta
PPV	Positive predictive value
ROC	Receiver operating characteristic curve
T2-Haste	T2-weighted half-Fourier single-shot turbo spin echo
T2-True FISP	T2-weighted true fast imaging with steady-state precession

Introduction

Abnormal invasive placenta (AIP) represents a spectrum of disease severity characterized by abnormal, firmly adherent placenta implantation with various depths into the uterus, which is typically referred to as placenta accreta, increta and percreta [1]. Prior caesarean section and placenta previa are important predisposing factors for AIP [2]. Over the past 40 years, the incidence of AIP has increased from <1/2000 in the 1980s to about 1/500 pregnancies at present, as a consequence of the concomitant increasing rate of caesarean section [1, 3].

When AIP occurs, the placenta may not be completely separated from the uterus at the time of delivery, resulting in potentially life-threatening intrapartum or postpartum massive haemorrhage and associated morbidity such as multisystem organ failure, disseminated intravascular coagulation and even death [4]. Placenta percreta (PP) is the most life-threatening invasion type of AIP, and is characterized by trophoblasts fully penetrating through the myometrium, including cases extending to or breaching the serosa and even invading surrounding structures [5]. A well planned multidisciplinary team approach could minimize the potential risks of maternal and/or foetal morbidity and mortality. Several studies have reported decreased morbidity (67.0% vs. 36.0%) and reduced blood loss (2,344 ± 1.7 vs. 2,951 ± 1.8 ml) in cases of prenatal planned caesarean sections, rather than emergent caesarean sections [1, 6, 7]. Thus, an accurate prenatal diagnosis of PP is imperative.

Although ultrasonography is the primary modality for antenatal diagnosis of AIP, placental MRI is playing an increasingly important role in preoperative planning [8]. Various MRI features have been shown to be indicative of AIP [9–14] and placental MRI has been reported to have good overall predictive accuracy in detecting AIP (sensitivity, 82.2–100%; specificity, 84.0–100%) [15–18]. However, distinguishing PP and placenta accreta (PA), especially in the absence of extauterine placental extension [19, 20], remains difficult. In addition, not only have some features (i.e. uterine bulge, placental bulge and abnormal vascularity) not been clarified in detail but also their diagnostic utility for reliably identifying pregnancies complicated by PP remains underexplored. Therefore, our primary objective was to identify specific MRI features for differentiating PP from PA and the secondary objective was to characterise the features of invasive placenta previa.

Methods

Patients

This retrospective study was approved by our Institutional Review Board, and written informed consent was waived. From January 2009 through March 2015, a total of 262 pregnant women with suspected invasive placenta previa (screened by ultrasonography) underwent prenatal placental MRI examinations at our institution. Ninety-three pregnant women with PA (mean gestational age, 33.4 weeks (range, 20–40 weeks); mean age, 32 years (range, 21–43 years)) and 45 women with PP (mean gestational age, 34.3 weeks (range, 22–39 weeks); mean age, 33 years (range, 20–42 years)) were recruited. All the PP patients had at least one prior caesarean section with an increased mean number of prior caesarean sections (1.3 (range 1–3)) than PA patients (1.1 (range, 1–2)).

The following clinical data were recorded: the rate of hysterectomy in PP and PA patients was 48.9% (22/45) and 17.2% (16/93), respectively; the rate of interventional therapy was 71.1% (32/45) and 63.4% (59/93), respectively; the blood loss during caesarean section in PP and PA patients was 3,137.8± 2,484.9 (800–15,000) ml and 1,490.3 ± 1,361.5 (200–8,000) ml, respectively. The detailed exclusion criteria and the study flowchart are shown in Fig. 1. No foetal or maternal sedation was used for any of the examinations, and specific absorption rate limits were in keeping with departmental protocols.

MRI examinations

The MRI examinations were performed on 1.5T MAGNETOM Amira (Siemens, Shenzhen Magnetic Resonance, Shenzhen, China) and MAGNETOM Sonata (Siemens, Erlangen, Germany) with body and spine array coils. All the patients were imaged in the supine position or left-lateral position with bladders moderately full. T2-weighted half-Fourier single-shot turbo spin echo (T2-Haste) and T2-weighted true fast imaging with steady-state precession (T2-True FISP) images were obtained without breath holding in the axial, coronal, sagittal and oblique sagittal planes. Additional imaging planes, perpendicular to the placenta-uterus interface or uterus-bladder interface, were obtained in the region of the suspected AIP. The acquisition parameters for all the sequences are shown in Table 1.

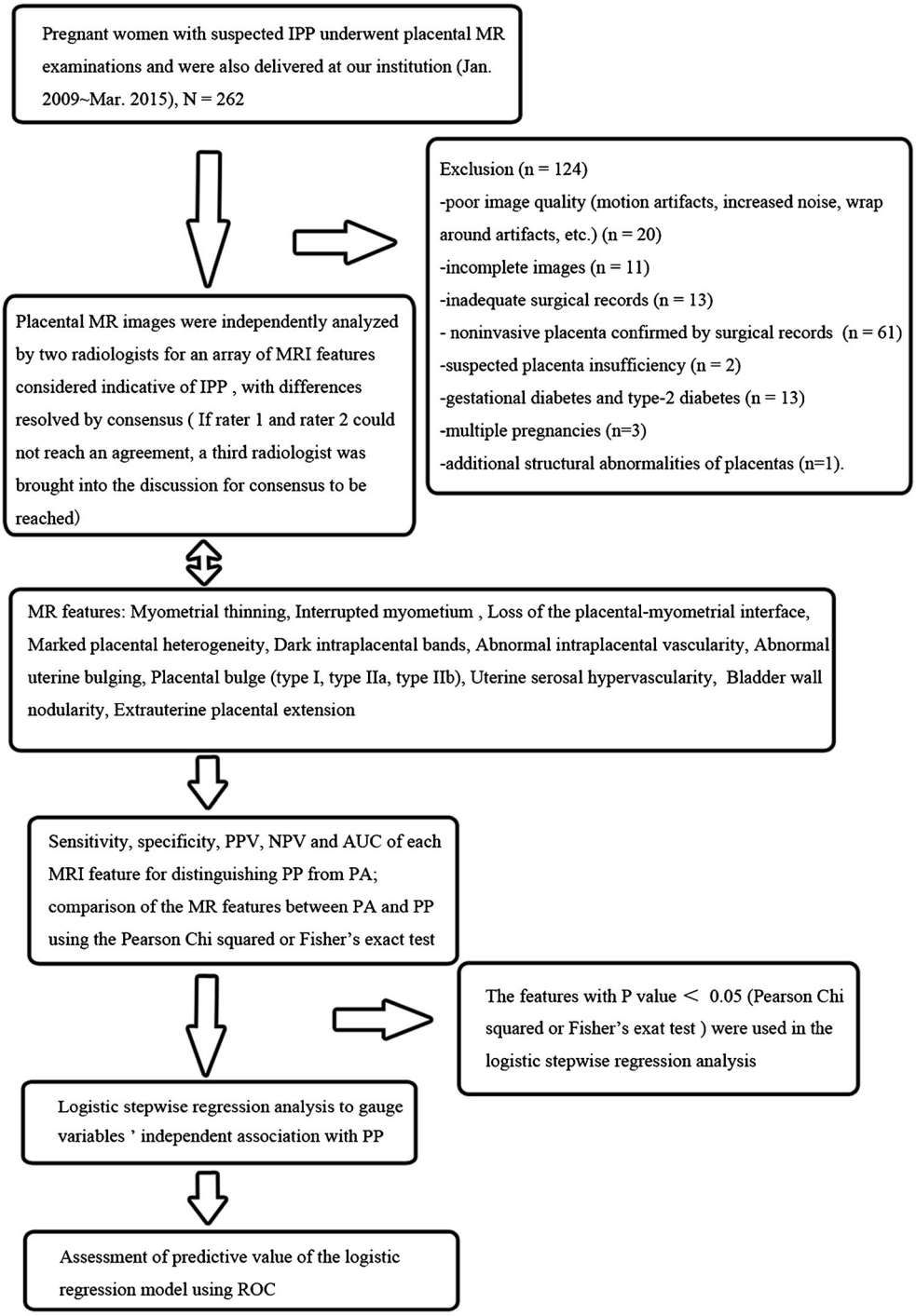

Note.— IPP = invasive placenta previa, PPV = positive predictive value, NPV = negative predictive value, AUC = area under the receiver operating characteristic curve, PA = placenta accreta, PP = placenta percreta, ROC = receiver operating characteristic curve

Fig. 1 Flowchart of the study design.

Standard of reference

Confirmation of PP was based on both surgical and pathological criteria: gross placenta/villi fully penetrating through the myometrium and invading the uterine serosa or even extrauterine structures [5, 9].

Confirmation of placenta accreta/increta was based on surgical and/or pathological evidence of placental adhesion to or invasion into the myometrium with intact uterine serosa [5, 20, 21]. The surgical evidence of PA also included the difficulty in manual removal of the placenta or massive bleeding after placental separation in a well-contracted uterus [9].

Table 1 Magnetic resonance imaging parameters

Parameter sequences	T2-Haste	T2-True FISP	T1WI	DWI(b=800)
TR/TE (ms)	1,000/94	4.3/2.1	286/4.62	5,000/97
Flip angle (degrees)	150	76	90	NA
Total acquisition time (s)	21–28	011–14	21	87
FOV (mm)	360–400	360–400	380	380
Slice thickness/gap (mm)	4–6/0.8–1.2	4–6/0.8–1.2	4–6/0.8–1.2	5/1.0
Voxel size (mm^3)	1.6×1.4×(4.0–6.0)	1.6×1.8×(4.0–6.0)	1.5×1.5×(4.0–6.0)	2.2×2.2×5.0
Acquisition matrix	256×256	256×256	256×256	176×176
NEX	1	1	1	4

T2-Haste T2-weighted half-Fourier single-shot turbo spin echo, *T2-True FISP* T2-weighted true fast imaging with steady-state precession, *DWI* Diffusion-weighted Imaging, *TR* repetition time, *TE* echo time, *FOV* field of view, *NEX* number of excitation, *NA* not applicable.

Imaging analysis

All the MR images were evaluated retrospectively on a Picture Archiving and Communication Systems work station by two experienced radiologists (Rater 1 and Rater 2, both with more than 5 years' experience in obstetric MRI reading), who were blinded to the original radiology reports and surgical and pathological information of the subjects. They evaluated all the MRI features independently for presence or absence, including the two types of placental bulge and the subtypes of placental type-II (type-IIa and type-IIb). If Rater 1 and Rater 2 could not reach an agreement, a third radiologist (Rater 3, with 7 years of experience of obstetric MRI reading) was brought into the discussion in order to reach a consensus. Prior to the image analysis, all the MR features were accurately defined and explained to all the raters. The MRI features considered indicative of invasive placenta previa were depicted as follows:

1. Myometrial thinning: The myometrium thins and the typical trilaminar appearance is undetectable [11].
2. Interrupted myometrium: The myometrium is interrupted abruptly at the site of focal placenta bulging [20].
3. Loss of the placental-myometrial interface: The thin hypointense layer disappears between the placenta and myometrium [11].
4. Marked placental heterogeneity: In the setting of intraplacental haemorrhage, infarct, abnormal vascularity or other parts of the abnormal signal are present, and the placenta signal is usually markedly heterogeneous [12, 22].
5. Dark intraplacental bands: These are depicted as nodular or linear areas of low signal intensity in the placenta on both the T2-Haste sequence and the T2-True FISP sequence. These bands are also characterized by having a maximum diameter of more than 2 cm, varying thickness, a random distribution, and extending from the uterine-myometrial interface to the intraplacental region [12].
6. Abnormal intraplacental vascularity: This is defined as tortuous enlarged flow voids on the T2-Haste sequence and high signal on the T2-True FISP sequence deep within the placenta-measuring at least 6 mm in diameter [10].
7. Abnormal uterine bulge: This feature is depicted as diffuse widening of the lower uterine segment, taking on an hourglass-shaped appearance [12, 20].
8. Placental bulge (type-I and type-II): Placental bulge is divided into two categories depending on whether the smooth uterine outline is distorted. When the placenta demonstrates a focal bulge slightly outwards into the subjacent myometrium and the outline is intact and not distorted, it is defined as placental bulge type-I; when the placenta shows a focal outward bulge with distorted outline shape and a blur of the subjacent outline, it is defined as placental bulge type-II. In our experience, bridging vessels are frequently noted through the focal bulging placenta (type-II). These bridging vessels are often running perpendicularly across through the focal bulging placenta and serosal layer, and extending to the parametrium. Therefore, we subdivided placental bulge type-II into two novel subsets: type-IIa (placental bulge with bridging vessels) and type-IIb (without bridging vessels). The above placental descriptors are illustrated in Fig. 2.
9. Uterine serosal hypervascularity: This represents tortuous and closely packed vessels (tortuous flow voids on the T2-Haste sequence and hyperintense on the T2-True FISP sequence) along the uterine serosa in the lower uterine segment on the axial images. These abnormal vessels are analogous to those seen on ultrasound [27].
10. Bladder wall nodularity: The bladder wall takes on an irregular or nodular hyperintense appearance [20].
11. Extrauterine placental extension: Placental tissues penetrate through the uterine serosa and form masses beyond the uterus [20].

Statistical analysis

For clinical relevance and statistical analysis, we used 'placenta accreta (PA)' as an umbrella term for placenta accreta

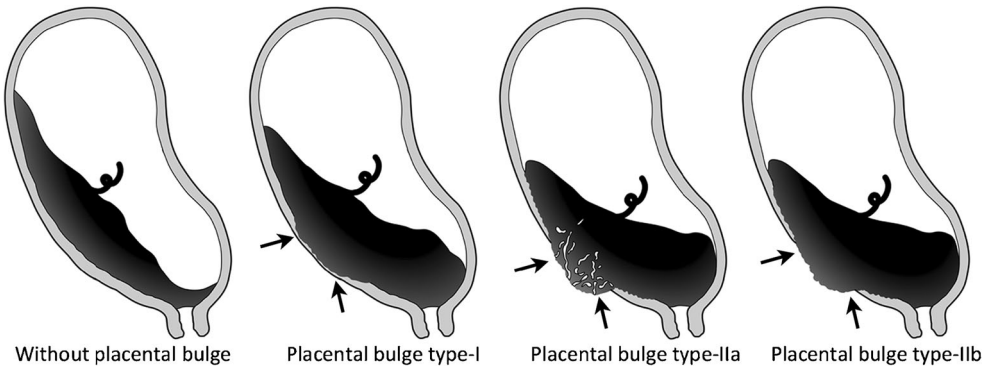

Fig. 2 Diagram illustrating the MRI features of placental bulge

and increta. Inter-rater agreement was evaluated by using *kappa* statistics. The sensitivity, specificity, positive predictive value (PPV), negative predictive value (NPV) and the area under the receiver operating characteristic curve (AUC) of each MRI feature were calculated. Moreover, all the potential MRI features were compared using Pearson's chi-squared or Fisher's two-sided exact test between women with PP and those with PA. Values that reached statistical analyses were then included in a logistic regression analysis to identify independent predictors of PP. A stepwise analysis was conducted using a forward stepping procedure based on a likelihood ratio test, with $P < 0.05$ for variable inclusion and $P > 0.1$ for exclusion from the model. The predicted value of the logistic regression model was assessed using the receiver operating characteristic (ROC) curve analysis. All the statistical tests were two-tailed, and $P < 0.05$ was considered to be statistically significant. The data were analysed using SPSS software (version 17, SPSS Inc., Chicago, IL, USA).

Results

Patient characteristics and clinical management

Of 138 women in the analysis, 45 had pathological and surgical confirmation of PP, and the remaining 93 women were diagnosed with PA (accreta/increta). Among the PA cohort, 57 (57/93) were confirmed by both surgical findings (at the moment of caesarean delivery) and pathological findings, and 36 (36/93) were confirmed by detailed surgical findings provided at the time of caesarean delivery. The increased number of prior caesarean sections was associated with higher risk for PP (P=0.038). The maternal characteristics of the entire study population are summarized in Table 2. The rate of hysterectomy in PP was higher than in PA ($P < 0.001$). The blood loss during caesarean section in the PP cohort was larger than that in the PA cohort ($P < 0.001$), regardless of the management methods used. There was no significant difference in the rate of interventional therapy between PP and PA (P=0.446), but the occluding time during interventional therapy in the PP cohort was longer than that in the PA cohort (36.4 ± 8.7 (25–65) vs. 25.1 ± 9.6 (11–50) min, $P < 0.001$). Among nine women with bladder involvement, eight of them underwent partial bladder resection and/or repair, and one had bladder cystotomy.

Inter-rater agreement

There was substantial agreement for all the MRI features of invasive placenta previa (*kappa* coefficient ranging from 0.661 to 0.801), except for myometrial thinning, loss of placental-myometrial interface and extrauterine placental extension. The detailed results are shown in Table 3.

Comparison of MRI features between placenta accreta (PA) and placenta percreta (PP)

Significant differences were found in nine depicted MRI features between pregnancies with PP and those with PA ($P<0.05$). However, only placental bulge type-II and uterine serosal hypervascularity yielded higher sensitivity (88.9% and 80.0%, respectively), higher specificity (90.3% and 73.1%, respectively) and a larger AUC (0.896 and 0.766, respectively) for differentiating PP from invasive placenta previa. Placental bulge type-I (Fig. 3) showed higher sensitivity (91.1%) but lower specificity (30.1%). Placental bulge type-IIa, bladder wall nodularity and extrauterine placental extension had 100% specificity and PPV, but the lowest sensitivity (37.8%, 20.0% and 2.2%, respectively). The detailed results are shown in Table 4.

Selection of the optimal MRI Features for distinguishing PP from PA

The nine significant MRI features were then introduced into a binary logistic regression analysis, which was used for selecting the optimal variables for distinguishing PP from PA. The MRI features of placental bulge type-II (Fig. 4) and uterine serosal hypervascularity (Fig. 5) were found to be independently associated with PP (odds ratio=48.618,

Table 2 Maternal characteristics and clinical information

Maternal demographics		Placenta accreta (n=93)	Placenta percreta (n=45)	P
Age, y*		32.2±4.6 (21–43)	33.4±5.0 (20–42)	0.115
Ethnicity, n (%)	Asian	93 (100.0)	45 (100.0)	1
Pregnancy BMI (kg/m^2)*		27.9±3.5 (19.2–37.5)	28.8±3.6 (22.6–40.8)	0.229
Gestational age (wk)†	at MRI	33 3/7 (20 1/7–40)	34 2/7 (21 5/7–39 3/7)	0.506
	at delivery	36 5/7 (21 0/7–40 4/7)	35 3/7 (23 0/7–39 4/7)	0.83
Placental previa	low lying or marginal partial	9 (9.7) 7 (7.5)	6 (13.3) 3 (6.7)	
	complete	77 (82.8)	36 (80.0)	
[a] Interventional therapy		59 (63.4)	32 (71.1)	0.446
	compression time (min)*	25.1±9.6 (11–50)	36.4±8.7 (25–65)	<0.001
Gravidity	mean (range)†	3.4 (2–8)	3.6 (2–8)	0.151
	2	33 (35.5)	6 (13.3)	
	3	22 (23.7)	17 (37.8)	
	4	18 (19.4)	14 (31.1)	
	≥5	20 (21.5)	8 (17.8)	
Prior caesarean delivery	mean (range)†	1.1 (1–2)	1.3 (1–3)	0.038
	1	81 (87.1)	33 (73.3)	
	2	12 (12.9)	10 (22.2)	
	3	0 (0)	2 (4.4)	
Blood loss at delivery, ml*		1,490.3±1,361.5 (200–8000)	3,137.8±2,484.9 (800–15,000)	<0.001
Hysterectomy performed		16 (17.2)	22 (48.9)	<0.001

Note: Placenta accreta and increta were considered together and are referred to as 'placenta accreta' Unless otherwise indicated, values are frequencies and numbers in parentheses are percentages

* Values are expressed as means ± standard deviations, with ranges in parentheses

† Values are means, with ranges in parentheses

Table 3 *Kappa* coefficients for assessment of inter-rater agreement for MRI features

MRI features	*Kappa*
Myometrial thinning	0.436
Interrupted myometrium	0.686
Loss of the placental-myometrial interface	0.491
Marked placental heterogeneity	0.665
Dark intraplacental band	0.777
Abnormal intraplacental vascularity	0.745
Abnormal uterine bulge	0.761
Placental bulge (type-I)	0.801
Placental bulge (type-II)	0.797
type-IIa	0.739
type-IIb	0.780
Uterine serosal hypervascularity	0.764
Bladder wall nodularity	0.661
Extrauterine placental extension	0.495

Note: The *kappa* coefficients were interpreted as follows: 0.00–0.20, slight agreement, 0.21–0.40, fair agreement,

0.41–0.60, moderate agreement, 0.61–0.80, substantial agreement, 0.81–1.00, almost perfect agreement

P<0.001; odds ratio=4.165, P=0.018, respectively), and were ultimately selected to form a logistic regression model (Table 5). Its accuracy for diagnosing PP was assessed using

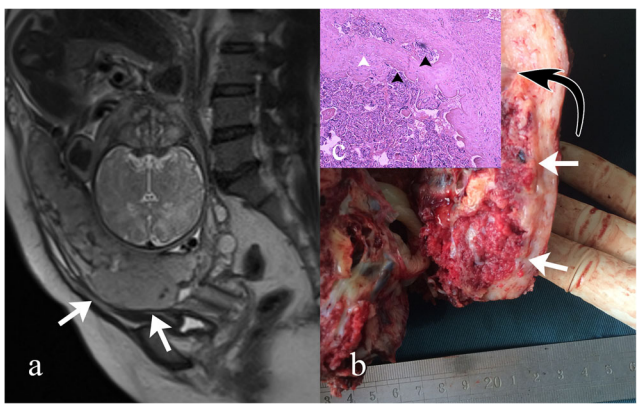

Fig. 3 Placenta increta (PI) in a 40-year-old woman at 35 weeks' gestation. (**a**) Sagittal T2-Haste MR image demonstrates placental bulge type-I (white arrows) with an intact uterine outline; (**b**) Photograph of gross specimens after hysterectomy shows placenta has invaded into the myometrium (white arrows) with intact uterine serosa, consistent with PI; (**c**) Photomicrograph (magnification, ×400; haematoxylin-eosin stain) shows chorionic villi (black arrowheads) implanted onto the myometrium (white arrowhead), consistent with PI

Table 4 Comparison of MRI features between placenta percreta and placenta accreta

	Placenta accreta (n=93)*	Placenta percreta (n=45)*	Sensitivity†	Specificity†	PPV†	NPV†	AUC	P
Myometrial thinning	93.6 (87)	100.0 (45)	100.0 (45/45)	6.5 (6/93)	34.1 (45/132)	100.0 (6/6)	0.532	0.177§
Interrupted myometrium	75.2 (70)	95.6 (43)	95.6 (43/45)	24.7 (23/93)	38.1 (43/113)	92.0 (23/25)	0.601	0.004‖
Loss of the placental-myometrial interface	96.8 (90)	100.0 (45)	100.0 (45/45)	3.2 (3/93)	33.3 (45/135)	100.0 (3/3)	0.516	0.551§
Marked placental heterogeneity	39.8 (37)	86.7 (39)	86.7 (39/45)	60.2 (56/93)	51.3 (39/76)	90.3 (56/62)	0.734	<0.001‖
Dark intraplacental band	53.8 (50)	88.9 (40)	88.9 (40/45)	46.2 (43/93)	44.4 (40/90)	89.6 (43/48)	0.676	<0.001‖
Abnormal intraplacental vascularity	62.4 (58)	93.3 (42)	93.3 (42/45)	37.6 (35/93)	42.0 (42/100)	92.1 (35/38)	0.655	<0.001‖
Abnormal uterine bulge	60.2 (56)	86.7 (39)	86.7 (39/45)	39.8 (37/93)	41.1 (39/95)	86.1 (37/43)	0.632	0.002‖
Placental bulge type-I	69.9 (65)	91.1 (41)	91.1 (41/45)	30.1 (28/93)	38.7 (41/106)	87.5 (28/32)	0.606	0.005‖
Placental bulge type-II	9.7 (9)	88.9 (40)	88.9 (40/45)	90.3 (84/93)	81.6 (40/49)	94.4 (84/89)	0.896	<0.001§
type-IIa	4.3 (0)	20.0 (17)	37.8 (17/45)	100 (93/93)	100 (17/17)	76.9 (93/121)	0.707	<0.001‖
type-IIb	5.4 (9)	68.9 (23)	51.1 (23/45)	90.3 (84/93)	76.7 (23/30)	79.2 (84/106)	0.689	<0.001‖
Uterine serosal hypervascularity	26.9 (25)	80.0 (36)	80.0 (36/45)	73.1 (68/93)	59.0 (36/61)	88.3 (68/77)	0.766	<0.001‖
Bladder wall nodularity	0.0 (0)	20.0 (9)	20.0 (9/45)	100.0 (93/93)	100.0 (9/9)	72.1 (93/129)	0.600	<0.001§
Extrauterine placental extension	0.0 (0)	2.2 (1)	2.2 (1/45)	100.0 (93/93)	100.0 (1/1)	67.9 (93/137)	0.511	0.326§

Note: Placenta accreta and increta were considered together and are referred to as 'placenta accreta'

PPV positive predictive value, *NPV* negative predictive value, *AUC* the area under the receiver operating characteristic curve * Values are percentages and numbers in parentheses are frequencies

† Numbers in parentheses are the data used to calculate the percentages

§ Fisher's test

‖ Chi-squared test

the ROC curve and the AUC was 0.92 (95% confidence interval: 0.92–0.98). When type-IIa and type-IIb (Fig. 4) served as dummy variables of placental bulge type-II, both of them were correlated with PP (β=23.47 and 3.39, respectively).

MRI features associated with abnormal vessels – correlation with blood loss during caesarean section

We also focused on the MRI features that were specifically associated with abnormal vessels (i.e. abnormal intraplacental vascularity, uterine serosal hypervascularity and bridging vessels) (Fig. 6).

In the PA cohort, women with the feature of abnormal intraplacental vascularity experienced greater blood loss during caesarean section than women without this feature ((1,730.2 ± 1,463.8 (200–8,000) vs. 1,092.9 ± 1,078.1 (200–4,000) ml, P = 0.030)); similar findings were noted when comparing the blood loss between women with and without the feature of uterine serosal hypervascularity ((2,044.0 ± 1,224.8 (400–5,000); 1,286.8 ± 1,360.7 (200–8,000, P = 0.010)). We also demonstrated that PP patients with the feature of placental bulge type-IIa (with bridging vessels) experienced greater blood loss during caesarean section than type-IIb (without bridging vessels) (3,829.6 ± 2,826.5.0 (1,000–15,000) vs. 2,192.3 ± 1,583.0 (800–5,000) ml, P = 0.016).

Discussion

In our study, placental bulge is initially subdivided into two types depending on whether the smooth uterine outline is distorted, and uterine serosal hypervascularity is preliminarily explored using MRI. The results of this study demonstrate that placental bulge type-II (with distorted uterine outline) and uterine serosal hypervascularity are specific MRI features for differentiating PP from PA. The MRI features associated with abnormal vessels (i.e. bridging vessels in placental bulge type-IIa, abnormal intraplacental vascularity and uterine serosal hypervascularity) appear to be risk signs for massive blood loss during caesarean section.

It has been previously reported that placental or uterine outward bulge was a useful sign of AIP [12, 19, 23], but the ability of this MRI feature to discern PP showed considerable variability [23–26]. Despite of two general descriptions of the bulge in previous studies (i.e. a diffuse bulge in the lower uterine segment resulting in an hourglass-shaped uterus [12, 19] and a focal placental bulge into the uterus [20]), the detailed classification and precise definition of the bulge were absent. In our study we classified the bulge on the basis of morphological characteristics on MRI images and explored their abilities to accurately diagnose PP.

Our results show that placental bulge type-II was the most discriminating MRI feature for reliably discerning PP from

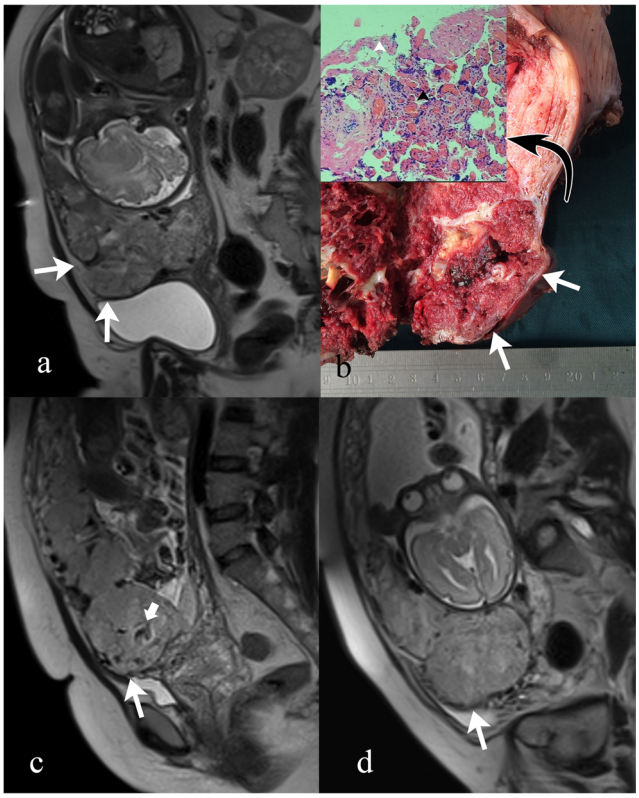

Fig. 4 (**a**-**b**) Placenta percreta (PP) in a 39-year-old woman at 30 weeks' gestation. (**a**) Sagittal T2-Haste MR image demonstrates placental bulge type-II (white arrows) protruding from the uterine outline; (**b**) photograph of gross specimens after hysterectomy shows placental invasion (white arrows) through uterine wall, consistent with PP; photomicrograph (magnification, ×400; haematoxylin-eosin stain) shows chorionic villi (black arrowhead) penetrating through the myometrium (white arrowhead), consistent with PP. Sagittal T2-Haste MR images show placental bulge type-IIa (long arrow, a focal outward bulge protruding from the uterine outline) with bridging vessels (short arrow) in a 31-year-old woman at 35 weeks' gestation with PP (**c**) and placental bulge type-IIb (long arrow) without bridging vessels in a 29-year-old woman at 32 weeks' gestation with PP (**d**)

invasive placenta previa, even when extrauterine placental tissues or the adjacent structure involvement was absent.

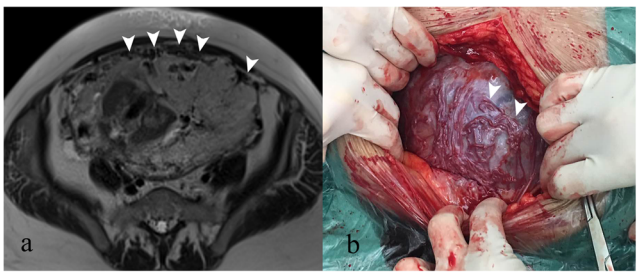

Fig. 5 Placenta percreta (PP) in a 35-year-old woman at 29 weeks' gestation. (**a**) Axial T2-Haste image demonstrates uterine serosal hypervascularity (arrowheads, tortuous and closely packed vessels along the uterine serosa) in the lower uterine segment. (**b**) Photograph taken during caesarean delivery shows these tortuous abnormal vessels in the uterine serosa (arrowheads), consistent with the appearance on MRI images

According to pathological examinations, the myometrium and the serosal layer were infiltrated by the chorionic villi at the area of the placental bulge type-II. Such infiltration decreases the strength and resiliency of the serosal layer and myometrium, which leads to focal distorted uterine outline. Based on this finding, placental bulge type-II could reflect the pathological change of PP. We further subdivided placental bulge type-II into two novel subtypes and found that placental bulge type-IIa (with bridging vessels) had 100% specificity and PPV. Therefore, the presence of this sign was reliable to diagnose PP. Of note, PP patients with type-IIa suffered more blood loss than type-IIb. These data suggested that these bridging vessels may increase the risk of massive haemorrhage, which may in part explain the difficulty in caesarean section among PP patients. However, abnormal uterine bulge and placental bulge type-I were found not to be discriminating variables for reliably discerning PP in our study. The detailed classification of the bulge was absent in the prior studies [25, 26], which may partly account for the variability in diagnosing PP.

Uterine serosal hypervascularity is a vital feature of ultrasound in diagnosing AIP [27–29]. However, to date this has not been examined using MRI. In our study, as a MRI feature, it was found to be notably correlated with PP, analogous to that seen on ultrasound [27]. Our results also showed that it was associated with larger blood loss during caesarean section. However, placenta previa and bladder varices are known to be associated with increased vascularity [10], which may bring about potential pitfalls. Although abnormal intraplacental vascularity was found not to be a capable feature in discerning PP, it is a risk sign of massive blood loss during caesarean section. Those profound abnormal vessels (bridging vessels in placental bulge-IIa, abnormal intraplacental vascularity, uterine serosal hypervascularity) can be explained by the pathological changes characterized by abnormal vascular architecture and plenty of arteriovenous shunts in the placental-maternal border [30]. These three types of abnormal vessels were in different regions of the placenta and/or uterus. Abnormal intraplacental vascularity is located deep within the placenta. Uterine serosal hypervascularity represents tortuous and closely packed vessels along the uterine serosa in the lower uterine segment. However, the bridging vessels are characterized by running perpendicularly across through the focal bulging placenta and serosal layer, and extending to the parametrium. With prior knowledge of these very abnormal vessels prenatally, obstetricians or interventional radiologists may attempt to safely perform devascularization of the involved area, which in turn would lead to reduced bleeding and a higher uterine preservation rate.

Consistent with previous studies [17, 20, 31], our study also found that bladder wall nodularity and extrauterine placental extension yielded the highest specificity and PPV but the lowest sensitivity, indicating that the two MRI features are highly suggestive of PP. The fact that the percentage of PP with invasion of the adjacent organs is not very high could account for its low sensitivity.

Table 5 Significant MRI features of logistic regression analysis for predicting the diagnosis of placenta percreta

	β	*p*	Odds ratio	95% CI odds ratio
Placental bulge type-II	3.884	<0.001	48.618	14.821–159.486
Uterine serosal hypervascularity	1.427	0.018	4.165	1.275–13.611

CI confidence interval

Early MRI criteria for diagnosing AIP have focused on evaluating direct invasion of the placenta into the uterus, including interrupted myometrium, myometrial thinning and loss of the placental-myometrial interface [13, 32]. Lax et al. [10] and Derman et al. [12] described several secondary MRI features associated with AIP. Although these features were more frequently detected in the patients with PP than those with PA [9], they did not accurately differentiate PP from PA.

Some studies have suggested that placental MRI with gadolinium could improve the ability to accurately diagnose AIP [33, 34]. But a new study published in JAMA found that gadolinium MRI during pregnancy was associated with an increased risk of a broad set of rheumatological, inflammatory, infiltrative skin conditions, etc. [35]. These contrast agents were not allowed to be routinely provided to pregnant women in our institution.

In our study, 23 patients with PP had uterine preservation. They benefitted from the conservative uterine-sparing surgery of placental-myometrial en bloc excision based on a well-established multidisciplinary team. This conservative surgery mainly included the devascularization procedure (preoperative placement of intra-arterial balloon catheters or uterine arteries embolization), placental-myometrial en bloc excision and uterine repair/reconstruction. In this surgery, the specimen of the intact placental-myometrial tissues (en bloc excision) is available, allowing the pathologists to evaluate the actual invasive depth.

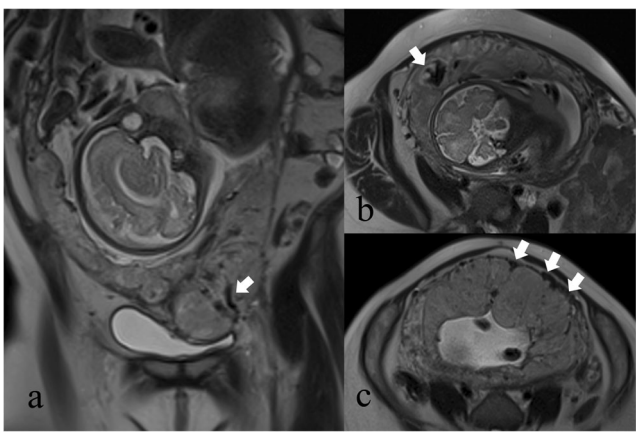

Fig. 6 (**a**) Coronal T2-Haste MR image demonstrates bridging vessels (arrow) through the bulging placenta in a 25-year-old woman at 32 weeks' gestation with placenta percreta (PP). (**b**) Axial T2-Haste MR image demonstrates abnormal intraplacental vascularity (arrow) in a 28-year-old woman at 30 weeks' gestation with placenta increta (PI). (**c**) Axial T2-Haste MR image demonstrates uterine serosal hypervascularity (arrows) in a 34-year-old woman at 35 weeks' gestation with PP

There are several limitations in this investigation that need to be addressed. Firstly, the inherence of the retrospective design of the study is inevitable. There is a need for further prospective studies in order to confirm the diagnostic applicability of the placental bulge type II and its subtypes. Another limitation is that all the MR examinations were performed on the population screened by ultrasonography. Therefore, there was a higher incidence of PP, which is likely to introduce a selection bias. Finally, we are aware of the fact that some cases of superficial placenta accreta may not be suspected, and also some superficial placenta increta may be misdiagnosed as placenta accreta by obstetricians during caesarean section. However, placenta accreta and increta were grouped together within the PA cohort in our study. Therefore, such misdiagnoses, if any, would not have altered the results. Forty-five cases of PP were confirmed by pathological and surgical criteria, which could enhance the diagnostic reliability of our study.

In summary, our results suggest that placental bulge type-II and uterine serosal hypervascularity are useful MRI features for differentiating PP from PA. Profoundly abnormal vessels are associated with larger blood loss during caesarean section. Our results may contribute to an accurate prenatal diagnosis of PP and minimum risk of massive haemorrhage.

Compliance with ethical standards

Guarantor The scientific guarantor of this publication is Guangbin Wang.

Conflict of interest The authors of this manuscript declare no relationships with any companies whose products or services may be related to the subject matter of the article.

Funding This work was supported by the National Natural Science Foundation of China under Grant No. 81371534, 81171380.

Statistics and biometry No complex statistical methods were necessary for this paper.

Ethical approval Institutional Review Board approval was obtained.

Informed consent Written informed consent was waived in this retrospective study.

Methodology
- retrospective
- comparative study
- performed at one institution

References

1. Belfort MA, S. c. f. M.-F. M. Publications Committee (2010) Placenta accreta. Am J Obstet Gynecol 203:430–439
2. Clark SL, Koonings PP, Phelan JP (1985) Placenta previa/accreta and prior cesarean section. Obstet Gynecol 66:89–92
3. Wu S, Kocherginsky M, Hibbard JU (2005) Abnormal placentation: twenty-year analysis. Am J Obstet Gynecol 192:1458–1461
4. Silver RM, Barbour KD (2015) Placenta accreta spectrum: accreta, increta, and percreta. Obstet Gynecol Clin North Am 42:381–402
5. Cunningham FG WJ (2010) Obstetrical hemorrhage. William's obstetrics, 23rd edn. McGraw-Hill, New York, pp 776–780
6. Eller AG, Porter TF, Soisson P, Silver RM (2009) Optimal management strategies for placenta accreta. BJOG 116:648–654
7. Warshak CR, Ramos GA, Eskander R et al (2010) Effect of predelivery diagnosis in 99 consecutive cases of placenta accreta. Obstet Gynecol 115:65–69
8. Palacios Jaraquemada JM, Bruno CH (2005) Magnetic resonance imaging in 300 cases of placenta accreta: surgical correlation of new findings. Acta Obstet Gynecol Scand 84:716–724
9. Bour L, Place V, Bendavid S et al (2014) Suspected invasive placenta: evaluation with magnetic resonance imaging. Eur Radiol 24: 3150–3160
10. Derman AY, Nikac V, Haberman S, Zelenko N, Opsha O, Flyer M (2011) MRI of placenta accreta: a new imaging perspective. AJR Am J Roentgenol 197:1514–1521
11. Kim JA, Narra VR (2004) Magnetic resonance imaging with true fast imaging with steady-state precession and half-Fourier acquisition single-shot turbo spin-echo sequences in cases of suspected placenta accreta. Acta Radiol 45:692–698
12. Lax A, Prince MR, Mennitt KW, Schwebach JR, Budorick NE (2007) The value of specific MRI features in the evaluation of suspected placental invasion. Magn Reson Imaging 25:87–93
13. Maldjian C, Adam R, Pelosi M, Pelosi M 3rd, Rudelli RD, Maldjian J (1999) MRI appearance of placenta percreta and placenta accreta. Magn Reson Imaging 17:965–971
14. Srisajjakul S, Prapaisilp P, Bangchokdee S (2014) MRI of placental adhesive disorder. Br J Radiol 87:20140294
15. D'Antonio F, Iacovella C, Palacios-Jaraquemada J, Bruno CH, Manzoli L, Bhide A (2014) Prenatal identification of invasive placentation using magnetic resonance imaging: systematic review and meta-analysis. Ultrasound Obstet Gynecol 44:8–16
16. Meng X, Xie L, Song W (2013) Comparing the diagnostic value of ultrasound and magnetic resonance imaging for placenta accreta: a systematic review and meta-analysis. Ultrasound Med Biol 39: 1958–1965
17. Masselli G, Brunelli R, Casciani E et al (2008) Magnetic resonance imaging in the evaluation of placental adhesive disorders: correlation with color Doppler ultrasound. Eur Radiol 18:1292–1299
18. Warshak CR, Eskander R, Hull AD et al (2006) Accuracy of ultrasonography and magnetic resonance imaging in the diagnosis of placenta accreta. Obstet Gynecol 108:573–581
19. Leyendecker JR, DuBose M, Hosseinzadeh K et al (2012) MRI of pregnancy-related issues: abnormal placentation. AJR Am J Roentgenol 198:311–320
20. Baughman WC, Corteville JE, Shah RR (2008) Placenta accreta: spectrum of US and MR imaging findings. Radiographics 28:1905–1916
21. Millischer AE, Salomon LJ, Porcher R, et al. (2016) Magnetic resonance imaging for abnormally invasive placenta: the added value of intravenous gadolinium injection. BJOG
22. Blaicher W, Brugger PC, Mittermayer C et al (2006) Magnetic resonance imaging of the normal placenta. Eur J Radiol 57:256–260
23. Rahaim NS, Whitby EH (2015) The MRI features of placental adhesion disorder and their diagnostic significance: systematic review. Clin Radiol 70:917–925
24. Cuthbert F, Teixidor Vinas M, Whitby E (2016) The MRI features of placental adhesion disorder–a pictorial review. Br J Radiol 89: 20160284
25. Thiravit S, Lapatikarn S, Muangsomboon K, Suvannarerg V, Thiravit P, Korpraphong P (2016) MRI of placenta percreta: differentiation from other entities of placental adhesive disorder. Radiol Med
26. Kilcoyne A, Shenoy-Bhangle AS, Roberts DJ, Sisodia RC, Gervais DA, Lee SI (2016) MRI of placenta accreta, placenta increta, and placenta percreta: pearls and pitfalls. AJR Am J Roentgenol 20:1–8
27. Cali G, Giambanco L, Puccio G, Forlani F (2013) Morbidly adherent placenta: evaluation of ultrasound diagnostic criteria and differentiation of placenta accreta from percreta. Ultrasound Obstet Gynecol 41:406–412
28. Jauniaux E, Collins SL, Jurkovic D, Burton GJ (2016) Accreta placentation: a systematic review of prenatal ultrasound imaging and grading of villous invasiveness. Am J Obstet Gynecol
29. Rac MW, Dashe JS, Wells CE, Moschos E, McIntire DD, Twickler DM (2015) Ultrasound predictors of placental invasion: the Placenta Accreta Index. Am J Obstet Gynecol 212:343 e341–347
30. Chantraine F, Blacher S, Berndt S et al (2012) Abnormal vascular architecture at the placental-maternal interface in placenta increta. Am J Obstet Gynecol 207:188 e181–189
31. Alamo L, Anaye A, Rey J et al (2013) Detection of suspected placental invasion by MRI: do the results depend on observer' experience? Eur J Radiol 82:e51–e57
32. Levine D, Hulka CA, Ludmir J, Li W, Edelman RR (1997) Placenta accreta: evaluation with color Doppler US, power Doppler US, and MR imaging. Radiology 205:773–776
33. Palacios Jaraquemada JM, Bruno C (2000) Gadolinium-enhanced MR imaging in the differential diagnosis of placenta accreta and placenta percreta. Radiology 216:610–611
34. Tanaka YO, Sohda S, Shigemitsu S, Niitsu M, Itai Y (2001) High temporal resolution dynamic contrast MRI in a high risk group for placenta accreta. Magn Reson Imaging 19:635–642
35. Ray JG, Vermeulen MJ, Bharatha A et al (2016) Association between MRI exposure during pregnancy and fetal and childhood outcomes. JAMA 316:952–961